Westward migration of oceanic ridges and related asymmetric upper mantle differentiation

Françoise Chalot-Prat, Carlo Doglioni, Trevor Falloon

Westward migration of oceanic ridges and related asymmetric upper mantle differentiation

Françoise Chalot-Prat[a], Carlo Doglioni[b], Trevor Falloon[c]

[a]*Centre de Recherches Petrographiques et Geochimiques – Lorraine University, BP20, 15 rue Notre Dame des Pauvres, F-54501 Vandoeuvre-les-Nancy Cedex, France.*

[b]*Dipartimento di Scienze della Terra, Sapienza University, P.le A. Moro, 5, 00185 Roma, Italy and Istituto Nazionale di Geofisica e Vulcanologia, Via di Vigna Murata 605, 00143 Roma, Italy*

[c]*School of Physical Sciences, Discipline of Earth Sciences, University of Tasmania, Hobart, Tasmania 7001, Australia*

Corresponding author: Françoise Chalot-Prat francoise.chalot-prat@univ-lorraine.fr

Highlights:

1. Westward ridge migration induces higher mantle refertilisation of the western plate ...88
2. Upwelling residual mantle is abandoned eastward consistent with seismological asymmetry ... 91
3. Ridge migration provides permanently MORB mantle source from the west ...73

Abstract

Combining geophysical, petrological and structural data on oceanic mantle lithosphere, underlying asthenosphere and oceanic basalts, an alternative oceanic plate spreading model is proposed in the framework of the westward migration of oceanic spreading ridges relative to the underlying asthenosphere. This model suggests that evolution of both the composition and internal structure of oceanic plates and underlying upper mantle strongly depends at all scales on plate kinematics. We show that the asymmetric features of lithospheric plates and underlying upper asthenosphere on both sides of oceanic spreading ridges, as shown by geophysical data (seismic velocities, density, thickness, and plate geometry), reflect somewhat different mantle compositions, themselves related to various mantle differentiation processes (incipient to high partial melting degree, percolation/reaction and refertilisation) at different depths (down to 300 km) below and laterally to the ridge axis. The fundamental difference between western and eastern plates is linked to the westward ridge migration inducing continuing mantle refertilisation of the western plate by percolation-reaction with ascending melts, whereas the eastern plate preserves a barely refertilized harzburgitic residue. Plate thickness on both sides of the ridge is controlled both by cooling of the asthenospheric residue and by the instability of pargasitic amphibole producing a sharp depression of the water-undersaturated solidus, its intersection with the geotherm at ~90 km, and incipient melt production right underneath the lithosphere-asthenosphere boundary (LAB). Thus the intersection of the geotherm with the water-undersaturated lherzolite solidus explains the existence of a low-velocity zone (LVZ). As oceanic lithosphere is moving westward relative to asthenospheric mantle, this partially molten upper asthenosphere facilitates the decoupling between lower asthenosphere and lithosphere. Thereby the westward drift of the lithosphere is necessarily slowed down, top to down, inducing a progressive decoupling within the mantle lithosphere itself. This intra-mantle decoupling could be at the origin of asymmetric detachment faults allowing mantle exhumation along slow-spreading ridges. Taking into account the asymmetric features of the LVZ, migration of incipient melt fractions and upwelling paths

from the lower asthenosphere through the upper asthenosphere are oblique, upward and eastward. MORB are sourced from an eastward and oblique, near-adiabatic mantle upwelling from the lower asthenosphere. This unidirectional mantle transfer is induced by isostatic suction of the migrating spreading ridge.

Key words

Asymmetric oceanic lithosphere, Westward drift of the lithosphere, Migrating ridge, Mantle melting, Percolation-reaction and refertilization, Detachment fault and mantle core complex, Secondary lherzolite and upper mantle differentiation

1. Introduction

The theory of plate tectonics, the post-1960's version of continental drift (Wegener, 1915), proposes that the lithosphere (crust + uppermost mantle) is divided into a number of plates that can move over, as well as descend into, the underlying asthenosphere and even deeper. However, since the development of plate tectonics theory, the link between geodynamics and the compositional differentiation of lithospheric and asthenospheric mantles has received relatively little attention. Most commonly, both plates and underlying asthenosphere are treated in geophysical modelling as closed systems evolving separately with little mutual interaction. Petrological and structural studies of exposed mantle lithologies and experimental petrology demonstrate significant interactions between lithospheric and asthenospheric mantles at mid-oceanic spreading ridges. Moreover in recent years, geophysical observations of oceanic plates have demonstrated a significant asymmetry of the oceanic lithosphere on both sides of oceanic spreading ridge axis (Doglioni et al., 2003; Muller et al., 2008; Panza et al., 2010 and references therein) in terms of seismic velocities, density, thickness, and plate geometry (Fig. 1). These observations are fundamental and require an explanation that integrates the whole data in order to improve our understanding of how the lithosphere and asthenosphere interact at and near spreading ridges.

Since the 1960s, plate tectonics is conceived as driven either by active mantle upwelling (‘bottom up’ or alternatively ‘ridge push’) or alternatively by the negative buoyancy of slabs (‘top down’ or alternatively ‘slab pull’). It is clear that creation of oceanic lithosphere and its subsequent subduction are fundamental mechanisms in governing the cooling of the Earth. In other words, the surface dissipation of both the Earth’s internal primordial and radiogenic heat is tied with the re-entrance of the cold lithosphere along subduction zones to determine the cooling of the planet. However, the mechanisms determining mantle drag and mantle convection remain a matter of debate. The asymmetry of subduction zones (those directed to the west are steeper and faster, e.g., Doglioni et al., 2007; Riguzzi et al., 2010) and plate motion reconstructions relative to the mantle reference frame support a westerly-directed drift of the lithosphere relative to the underlying mantle, also called net rotation (as a mean value) or westward drift (Wegener, 1915; Holmes, 1944; Carey, 1958; Le Pichon, 1968; Bostrom, 1971; Moore; 1973; Ricard et al., 1991; Gripp and Gordon, 2002; Crespi et al., 2007; Cuffaro and Doglioni, 2007). The net rotation or the westward drift of the lithosphere requires both a decoupling at the lithosphere-asthenosphere interface and a mechanism driving this rotation (Doglioni et al., 2011; Doglioni and Anderson, 2015; Doglioni and Panza, 2015). The motion is not east-west, but along an undulated flow that varies from WNW to E-W to ENE trends, along the so-called ‘tectonic equator’ (Crespi et al., 2007). Proposed mechanisms involve either the negative buoyancy of the lithosphere (Ricard et al., 1991), or the astronomical drag induced by the Earth’s rotation

combined with tidal friction (Riguzzi et al., 2010). Potentially astronomical forces may interact with mantle convection resulting from the cooling of the Earth (Holmes, 1944; Carey, 1958; Scoppola et al., 2006).

The aim of our paper is to build an oceanic spreading model integrating existing compositional, structural and geophysical data across oceanic ridges and the underlying upper mantle. We show the interdependence between the oceanic spreading process, the upper mantle differentiation and plate kinematics driven by the westward drift of the lithosphere. Our model enables to integrate, in space and time, natural and experimental petrology results on upper mantle differenciation (down to 300 km depth) and oceanic, tholeiitic and alkalic, basalt genesis (Green et al., 2014; Green 2015; Green and Falloon, 2015 and references therein), and provides a mechanism for upper mantle geophysical stratification with lateral heterogeneity as evidenced by Thybo (2006).

We will use the well accepted terminology of geophysicists, i.e., upper asthenosphere as the equivalent of "petrological' asthenosphere" corresponding to the Low-Velocity Zone (LVZ), and lower asthenosphere as the equivalent of "petrological' sub-asthenosphere" that reaches about 410 km of depth (Green and Falloon, 1998). They are defined in terms of depth, thickness and composition later in this paper.

2. Asymmetry on both sides of oceanic spreading axis and preliminary model

Since the recognition of magnetic anomalies on both sides of oceanic ridges (Vine and Matthews, 1963), oceanic rift zones were considered as having symmetric features, and plate spreading as a symmetric geological process. As shown by Doglioni et al. (2003), observations on the bathymetry of ridge flanks (shallower eastward) of Pacific and Atlantic oceans and on variable rates of oceanic spreading (Muller et al., 1997; 2008; Mallows and Searle, 2012) contradict the concept of full symmetry. Panza et al. (2010) and Panza and Romanelli (2014) provided evidence for asymmetry in both shear wave velocity and thickness within mantle lithosphere and asthenosphere when comparing the two sides of most spreading ridges. In general, the old (>60 Ma) western lithospheric plates have a faster shear wave velocity and are thicker (≈100 km versus ≈80 km in the eastern flank). Seismic tomography (Thybo, 2006; Panza et al., 2010; Schmerr, 2012; Panza and Romanelli, 2014) provides robust evidence of an asymmetric LVZ at depths from about 80-100 km down to 180-225 km. The average Vs within the western LVZ is slower than the eastern one. The LVZ shape is itself asymmetric, being thicker and wider on the western side of ridges. Also passive continental margins and the related continent-ocean transition support a systematic asymmetry of rift zones (Lavier and Manatschal, 2006; Brune et al., 2014).

All these asymmetric features appear to be independent from the age of the oceanic lithosphere, although they become more prominent moving toward older lithospheric ages (Panza et al., 2010). These observations suggest that mantle compositions and related physical parameters such as rigidity μ, density ρ and their ratio μ/ρ, are systematically different from one side to the other of a spreading ridge within both the lithosphere and the upper asthenosphere, i.e., the LVZ.

Panza et al. (2010) explain these observations as a result of the depletion of the upper asthenosphere, that evolves from pre-melting lherzolite into post-melting harzburgite composition below the oceanic ridge, while the ridge is moving westward relative to the asthenospheric mantle, i.e., in the hot-spot reference frame (Crespi et al., 2007). The role of ridge migration (Scheirer et al., 1998; Small and Danyushevsky, 2003; Doglioni and Panza, 2015) in producing an oceanic plate asymmetry is a key parameter of the model. To the east of the ridge, the lithospheric mantle (named also LID) would represent the residual product from partial melting of upwelling asthenosphere,

abandoned and in the process of cooling after the ridge migration to the "west". Since ridges are shifting above a fertile asthenospheric mantle, there is a continuous supply of MORB source mantle beneath the migrating spreading ridge (Panza et al., 2010). This model, deduced from geophysical and kinematic data (Fig. 1), suggests that the westward drift of the lithosphere relative to the underlying asthenosphere is a global phenomenon, a concept that implies decoupling between lithosphere and asthenosphere occurring within the LVZ, i.e., in the upper asthenosphere.

Important questions that arise from the above observations are as follows:

i) How does oceanic lithospheric mantle form?

ii) How can the mantle lithosphere composition evolve differently on each side of the ridge?

iii) How to combine oceanic spreading and westward drift of the lithosphere? Could the detachment-mode of seafloor spreading (Maffione et al., 2013; Whitney et al. 2013 and references therein), be the visible major effect in the field?

iv) How does asthenosphere evolve in relation with oceanic lithosphere during plate spreading? What controls the differentiation between lower and upper asthenosphere and the rather homogeneous thickness (≈125km) of the upper part?

v) How to combine the ascent of MORB source mantle from the lower asthenosphere according to experimental P-T-depth conditions (Green et al., 2014) with oceanic spreading and westward drift of the lithosphere?

vi) Is the oceanic lithosphere denser than the underlying asthenosphere?

3. Deciphering the compositional and physical evolution of the oceanic lithospheric mantle on both sides of a spreading ocean ridge

Lithospheric plates of slow spreading oceans (up to 4cm/yr, e.g., Atlantic, Arctic, southwest Indian and Antarctic) are known to be mostly composed of mantle rocks. Volumes of extrusive and intrusive magmatic rocks, representative of the magmatic oceanic crust, remain minor (Cannat, 1993; Chalot-Prat, 2005; Smith et al., 2008, 2012). Lithospheric mantle is thus the main component of the oceanic plate, which reinforces the major role of oceanic mantle for understanding the nature and construction of the ocean floor. For this reason the following discussion (below) will focus firstly on the physical then secondly on the petrological features of the lithospheric mantle.

3.1. General physical features and composition of oceanic lithosphere

The oceanic lithosphere is deeply fractured at the ridge axis. This major fracture network reaches the top of the ductile layer in the lithosphere, and two plates, A and B, form and spread apart. The western plate A always moves westerly faster than the eastern plate B (Fig. 2) as shown by Crespi et al. (2007). In our model, due to the westward drift of the lithosphere (Le Pichon, 1968; Doglioni et al., 2003), both plates move to the west, the western plate A at V_A and the eastern plate B at V_B, being $V_A > V_B$ (Fig. 2). The oceanic ridge moves west at $Vr = (V_A + V_B)/2$. Plate growth rate is due to the difference between V_A and V_B. Thus the separation between points on each plate increases at the half spreading rate (hS) which is given by $(V_A - V_B)/2$. Vr is always faster than hS.

The thickness of the oceanic lithosphere can be estimated from geophysical data including seismic, gravity, and electrical conductivity It can also be inferred from geotherm/lherzolite solidus intersection based on experimental studies at controlled P, T and water contents.

Geophysical data show lithospheric thickness decreasing towards ridge axes above shallowing asthenosphere. However we do not think that the lithosphere-asthenosphere boundary (LAB) reaches the base of the newly formed basaltic crust at fast spreading ridges, nor approaches the sea floor at

magma-starved slow-spreading ridges. This view is based on the petrology (phase assemblages), chemical compositions and isotopic compositions of peridotites sampled from rifted margins, ridge/transform intersections and slow-spreading ridges. Only lithospheric (secondary harzburgite or secondary lherzolite; see Piccardo et al., 2007b), but not asthenospheric mantle compositions have been identified either at the bottom of rift axis in slow-spreading active and fossil oceans (e.g., Seyler and Bonatti, 1997; Dijkstra et al., 2001; Takahashi, 2001; Tartarotti et al., 2002; Müntener et al., 2004; Piccardo et al., 2004, 2007a b, 2014; Kaczmarek and Müntener, 2008, 2010; Rampone et al., 1997, 2005, 2008; Rampone and Borghini, 2008; Warren and Shimizu, 2010; Muntener et al., 2010; Piccardo and Garnieri, 2010; Rampone and Hofmann, 2012; Warren, 2016), or below oceanic crust in fast-spreading active and fossil oceans (Dick and Natland, 1996; Abily and Ceuleneer, 2013). The depth of the LAB under the ridge may be inferred in two ways: 1. estimating the depth of melt segregation for parental MOR picrites or basalts and 2. by the P, T conditions recorded in ridge peridotites (including their P, T decompression paths in some cases). Indeed experimental results (Fig. 3) demonstrate that parental MOR picrite segregation from residual peridotite occurs mostly between 2 to 1.6 GPa (up to 2.2 GPa; down to 1.1 GPa), thus between 55 to 45 km depth (down to 65 km; up to 30 km), around 1400°C (up to 1430°C) from a trace element depleted lherzolite (Eggins, 1992a,b; Falloon et al., 2007a,b; Green et al., 2001; Green and Falloon, 2005; Green et al., 2014; Green and Falloon, 2015). Magma genesis produces mantle residual peridotite less dense than the asthenospheric protolith, accreting above its asthenospheric source and potentially subject to percolation-reaction of new magma ascents, giving birth to a refertilized constantly growing oceanic lithospheric mantle. From experimental results on liquid compositions in equilibrium with spinel and/or plagioclase lherzolite assemblages (Falloon et al., 2007a, b; Chalot-Prat et al., 2010; 2013), analogous to natural oceanic mantle samples, the oceanic lithospheric mantle thickness at the ridge is at least 20 km and up to 40 km in thickness. Note that density differences are due to chemical/mineralogical differences but also to temperature differences (e.g., residual mantle temperature has been reduced by the lost of the latent heat of melting). Thus determining density differences is subject to significant uncertainties.

Laterally on both sides of the ridge axis, seismic data show a progressive thickening of oceanic mantle lithosphere until around 80-100 km maximum, equivalent to 3 GPa of pressure. This thickening is assumed to derive first from the addition of the cooled uppermost part of asthenosphere (below 1100°C; Green and Falloon, 2005; Green et al., 2014). Green and Falloon (2005) and Green et al. (2010, 2011, 2014) have shown experimentally that the lithospheric mantle thickness depends on its water storage capacity (Fig. 3). Indeed at pressures greater than 2.5 to 3 GPa (80 to 100 km depth), instability of pargasite causes a sharp drop in the water storage capacity of fertile lherzolite, and for water content greater than ~ 200 ppm in the lithosphere, the mantle solidus is depressed at 2.5-3 GPa along the geotherm. In both cases partial melting can explain both the thickness of the oceanic lithosphere and the occurrence of a LVZ just below the LAB. Therefore from a petrological point of view, the LAB detected by the slowing of seismic waves is the intersection of the geotherm with the vapour-undersaturated lherzolite solidus, and the LVZ is a layer in which there is incipient melt (probably <1-2 % melt).

As far as it concerns the depth/temperature of the base of the oceanic lithosphere outside the ridge (>500 km), the model of Afonso et al. (2007) predicts 1300°C at 105 km depth. This temperature is somewhat too high according to experimental data of Green et al. (2010, 2014), showing that a “wet” (>200 ppm H_2O) oceanic lithospheric mantle is above its solidus below 80-100 km if temperature is higher than 1000 °C (Fig. 3). Below this depth, this is the LVZ, thus the upper asthenosphere. An incipient melt is present, the melt fraction being determined primarily by the water and CO_2 contents.

219 This melt has low permeability (i.e. can only move slowly by porous flow), but has a large effect on
220 seismic and rheological properties.

221 *3.2. How oceanic mantle lithosphere of the western limb of the ridge axis becomes thicker and denser*
222 *compared to the eastern limb?*

223 *3.2.1 Intra-lithospheric mantle decoupling*
224 In this section we will focus on the modalities of mantle mass transfer upwards and laterally within
225 both spreading plates in the framework of the westward drift of the lithosphere. Oceanic mantle
226 lithosphere is created at the ridge through accretion of residues above the asthenospheric partial
227 melting area. These residues are successively transferred upwards and laterally at hS rate within the
228 mantle lithosphere on each side of the ridge (Fig. 2). As Vr is higher than hS, the transfer rate of
229 successive residues above the melting area is slower than the westward velocity of the melting area
230 itself. Accordingly, mantle exhumed at the bottom of any active axial ridge is always older than the
231 basaltic volcanoes emplaced at the axial ridge (Bonatti et al., 2003). It is the same for intrusive gabbro
232 bodies which move upwards and laterally, driven by and with the upwelling of the host-mantle: for
233 instance, for hS=2cm/yr, Vr=4cm/y and a mantle residue initial depth of Di=40 km, the mantle residue
234 takes t1 2 Ma (t1=Di/hS) to ascend and to be exhumed at the surface. Thus active volcanoes at the
235 ridge axis are about 2 Ma younger than the mantle on which they are formed. Besides, while this
236 mantle residue is rising up to the ocean floor, the ridge itself with the uppermost part of the
237 lithosphere will have moved (t1*Vr) 80 km westward. However it may be possible that due to
238 'second-stage melting', the extra buoyancy added to the residue may accelerate the upwelling – in
239 which case some residue may be younger than 2Ma.
240 Therefore, besides the notion that asthenosphere is moving "eastward" relative to the lithosphere
241 (or more precisely along the flow lines parallel to the undulate tectonic equator of Crespi et al., 2007
242 and Cuffaro and Doglioni, 2007), the westward drift of the lithosphere is necessarily slowed down,
243 top to down, inducing a decoupling within the mantle lithosphere itself. This is visualized on the
244 model (Fig. 2) with the progressive top-down eastward shifting of the "half-spreading residues"
245 relative to each other within both plates. This decoupling would be progressive such that the top of the
246 melting area would be somewhat delayed relative to the top of the axial ridge, even if they are
247 interdependent.

248 Normal faults are the natural feature associated with rift zones and as indicated by rock mechanics,
249 their mean dip is around 60°. Lower dips may naturally result from a decrease of friction due to the
250 high heat flow and moving into shear zones within the underlying ductile layer. Besides faults and
251 fractures may dip predominantly in one direction if spreading is asymmetric. Indeed the half spreading
252 rate is often slighlty asymmetric (Mueller et al., 2008), but this is related not to the velocity of plates
253 relative to the mantle, but to the velocity of the ridge which sometimes is not exactly $(V_A+V_B)/2$; it
254 may be $(V_A+V_B)/1.95$ or $(V_A+V_B)/2.05$ etc. Therefore faster and larger spreading may occur in one
255 flank without varying the relative velocity of the two plates with respect to the mantle. This can be
256 explained by the lateral viscosity variations in the flanks right beneath the ridge. Therefore, ridge-
257 related faults and associated fractures would dip mainly "eastward" and be convex upwards since the
258 westward drift is faster upwards, but their dip may also be opposite due to the half-spreading process.
259 This is the geometry of detachment faults, i.e., large offset low-angle faults capping the eastern (rarely
260 western) side of oceanic mantle core complexes (OCC ; Smith et al., 2008, 2012; MacLeod et al.,
261 2009; Reston and Ranero, 2011; Mallows and Searle, 2012; Whitney et al., 2013; Maffione et al.,
262 2013) and extending along steep faults probably rooted in a melt-rich zone. They are responsible for

exhumation of mantle and plutonic rocks onto the seafloor in the footwall of normal faults, whereas extrusion of basalt occurs on the hanging wall.

This intra-mantle decoupling within the lithosphere means also that even a mid-oceanic ridge and its related fracture network shift probably westward within the lithosphere, moving itself westward relative to the asthenosphere. This cannot be visible from the surface, and this is why general symmetry of magnetic stripes on the oceanic sea floor is preserved. However Carbotte et al. (2004) and Mallows and Searle (2012) note a westward shift of volcanic activity with time along the active Mid-Atlantic ridge axis. The geological maps of Mallows and Searle (Fig. 4; 2012) and Smith et al. (Fig. 4; 2012) show that most OCC outcrops on the western side of the ridge and that spreading rates are asymmetric with faster spreading on western plates. According to Whitney et al. (2013 and references therein), OCC account for 60% to 100% of the total plate spreading, showing that tectonic process is the main driver of mantle exhumation in the oceans and of heat and mass transfer in the Earth. Furthermore, Maffione et al. (2013) introduce the concept of detachment-mode of seafloor spreading. Moreover, the usual sill shape of gabbro intrusive bodies both at multimetric and multikilometric scale (Henstock et al., 1993 and references therein; Chalot-Prat, 2005) testifies sub-horizontal magma injections within weakness zones of lithospheric mantle, supporting intra-mantle decoupling during ocean spreading. Volcanoes grow on the topmost part of the hangingwall of these large detachment faults, structuring hangingwall rider blocks (Whitney et al., 2013; Maffione et al., 2013 and references therein). Small-scale decoupling occurs between the base of volcanoes just emplaced and underlying mantle or/and gabbro bodies in the process of exhumation. This decoupling occurs on both sides of relief where eruptions take place, underlining a pseudo-symmetric spreading (Chalot-Prat, 2005).

3.2.2. Asymmetric evolution of lithospheric mantle compositions and physical parameters on each side of the ridge

The variation of Vs between the two sides of the oceanic ridge should have an explanation in terms of composition related to the different kinematics. As the melting area moves westward with the migrating spreading axis, the eastern plate B incorporates successively the abandoned depleted eastern parts of the ridge. It undergoes a relatively brief time of refertilization by ascending MORB and its composition remains close to a harzburgitic residue and is relatively Fe-poor. At the same time, harzburgitic residues are also continuously added to the western plate A, but, in contrast to the eastern plate, they are also continuously percolated by MORB as the ridge is moving westward above the underlying melting area linked to the ridge location. Thus the composition of the western plate A is that of a strongly refertilized harzburgite, thus a secondary lherzolite. An outcropping example could be the lherzolites from the Lanzo oceanic mantle area (Piccardo et al., 2007, and references therein). Therefore lithospheric mantle of the plate A is continuously re-enriched in Fe and Ca, whereas lithospheric mantle of the plate B remains a harzburgitic residue barely re-enriched in Fe and Ca.

Nevertheless as Vr>hS, the axial ridge is moving westwar within the lithosphere itself, and the western plate A is progressively incorporated within the eastern plate B. This means that the plate B composition will become somewhat more refertilized than presented above. However the overall consequence is that the western plate A is thicker, always richer in Fe and thus denser than the eastern plate B, resulting in a first order asymmetry in composition between the two plates.

In addition, if the westward drift is producing intra-lithospheric deformation preferentially on the western plate – then we might expect easier and more abundant pathways for off-axis magmatism and hence off-axis melt impregnation and channelling. Some of the upwelling diapirs may lose part of their melt fraction before arriving directly under the ridge axis. Evidence for this could be an

asymmetry in abundance of off-axis seamounts (i.e. volcanic chains on western plate as in Shen et al., 1993, White et al., 1998). If this off-axis process occurs – then there will be less melt arriving directly under ridge axis – and hence the eastern flank will receive long-term less fertilised residue than the western flank.

is higher than ρB (previous paragraph), μA must be much higher than μB. Since the modulus of rigidity of Fe is around 3 to 4 times higher than that of Mg and Si, the rigidity of rocks is expected to be enhanced if they are richer in Fe-rich minerals (Fyfe, 1960; Jordan, 1979). Thus higher μA compared to μB is an expected natural consequence of enhanced melt refetilization under the western plate A during westward migration of the spreading ridge.

4. Deciphering the physical and compositional evolution of the asthenosphere below a spreading oceanic lithosphere

4.1. Lower asthenosphere

The lower asthenosphere is subsolidus garnet lherzolite, about 180 km thick (230 to 410 km depth) overlying the Transitional Zone beginning at ~ 410 km (Anderson, 2007; 2010; Schmerr, 2012). From the top to the bottom of this layer, seismic waves gradually increase their speed with respect to the LVZ. Vs is much higher than in the upper asthenosphere and more or less similar to that of the lithosphere (Panza and Romanelli 2014). Its mineralogical and chemical composition is inferred from experimental petrology on MORB genesis (Green et al., 2014; Green, 2015), being the N-MORB mantle source located below 230 km. It is a fertile garnet lherzolite, depleted in the most incompatible trace elements, with ≥200 ppm H_2O and with incipient melt at ≤ 7 GPa/~230 km, 1490°C. As shown in Fig. 3, an oceanic intraplate geotherm joins the mantle adiabat at about 230 km depth defining the base of the upper asthenosphere. The lower asthenosphere may migrate upwards as diapirs within the 230-100 km including very small, relatively immobile, near-solidus melts (0.05–0.1 % of melting).

4.2. Upper asthenosphere

Within the upper part (80-220 km depth) of the asthenosphere, i.e., the LVZ, Vs is slower in the western than in the eastern side of the ridge, the reverse of what it is observed in the oceanic lithosphere (Panza et al., 2010). We infer that during its transfer from west to east below the oceanic lithosphere, the eastern part of upper asthenosphere becomes somewhat Fe-depleted by incipient melting (Fig. 2) inducing a density decrease for a potentially similar value on rigidity from one side to the other of the axis. Moreover as shown by experiments of Conder and Wiens (2006), Hammond and Toomey (2003) and Green et al. (2014), the western part of the upper asthenosphere is hotter and/or richer in H_2O+CO_2 than its eastern part and includes higher melt fractions inducing a rigidity decrease in the western side. It follows that to the "west" of a spreading ridge, both the oceanic lithospheric mantle (down to 90-100 km) and the upper asthenosphere (down to 230 km) should be more fertile and denser than the "eastern" part. Let us remember that in both mantle layers, density is determined not only by mantle fertility and Fe-enrichment, but also by the pargasite content in the lithospheric mantle and by percentage of melt within the upper asthenospheric mantle.

The LVZ has been seismically recognized below all oceans, both beneath the "western" and the "eastern" plates. It has a very small aspect ratio (thickness: 130 km; length in spreading direction: $6*10^3$ km below the Atlantic to $11*10^3$ km below the Pacific). Experimental results (Fig. 3) show that the upper asthenosphere corresponds petrologically to a mantle layer including small interstitial melt fractions (i.e. 0.05 to 0.1 %). According to Doglioni et al. (2005), the degree of partial melting would

503 be increased (up to 1.5 %) by shear heating (more than 100°C) generated by decoupling between
504 lithosphere and lower asthenosphere (Fig. 3) and with largest contribution i.e. largest E-W relative
505 movement at ~230 km depth. It may be alternatively due to higher H_2O content in the mantle (Bonatti,
506 1990; Ligi et al., 2005).
507 Moreover, seismic images from Panza and Romanelli (2014) show an asymmetric shape of the
508 LVZ, thicker and more elongated westward (2/3 in volume) than eastward (1/3 in volume) of ridge
509 axis in all oceans. This spectacular and permanent asymmetry of the LVZ shape raises the question
510 not only of the origin of partial melting, but also of its much greater development below the western
511 part of the oceans. From experimental results (Fig. 3), the presence of these very small melt fractions
512 have two distinct origins depending on the H_2O content of the mantle sources: 1- below the
513 lithosphere-asthenosphere boundary (LAB) and far away from the ridge (>500 km): because of
514 destabilization of amphibole, below 2.5-3 GPa/ 80-100 km/ 1000-1100°C, when "wet" (>200 ppm
515 H2O) oceanic mantle lithosphere, i.e. a subsolidus pargasite-bearing garnet lherzolite cools, subsides
516 and becomes asthenosphere, i.e. a pargasite-out garnet lherzolite with incipient melting. 2- above the
517 lower-upper asthenosphere boundary: during adiabatic (≈1490-1450°C) "dry" (<200 ppm H2O) ascent
518 of the lower asthenosphere from ≥230 km/ ≥7 GPa towards the MORB genesis area, i.e. 65-45 km/ 2-
519 1.6 GPa below the ridge axis. Let us note that if the first partial melting origin corresponds to a rather
520 static process linked only to the permanent thickening of the lithospheric mantle, the second is
521 synchronous with a dynamic process of partially molten transfer of matter, both being imaged by the
522 LVZ.
523 In parallel, the LVZ asymmetry suggests that the on-going ascent of partially molten mantle from
524 lower asthenosphere is oblique, and not vertical, as already proposed by Carbotte et al. (2004). Taking
525 into account its dimension, the ascent would be initiated around some thousands kilometers “west”
526 from the ridge (Fig. 2), and driven by a suction effect towards the shallow area below the spreading
527 ridge moving “westward”, due to the removal of the overlying lithosphere and the consequent
528 asthenospheric isostatic compensation.
529 Nevertheless according to the entrance angle of lower asthenosphere into upper asthenosphere, this
530 lateral and upward mass transfer is more or less counteracted by the relative “eastward” horizontal
531 mantle flow linked to the net rotation of the lithosphere, whose origin can be ascribed either to lateral
532 viscosity variation (e.g., Ricard et al., 1991) or to the Earth’s rotation (Scoppola et al., 2006; Riguzzi
533 et al., 2010). Two different paths of transfer would exist. The main path involving the largest mantle
534 volume follows a very low angle trajectory, barely deviated in passing below the spreading ridge; it
535 would concern the mantle flux emerging rather far laterally (more than 500 km?) from the spreading
536 centre. From experimental results (Fig. 3), this mantle flux crosscuts the intraplate geotherm, modified
537 by shear heating, and undergoes incipient to low degrees of partial melting (up to 4% down to 80-100
538 km deep / 2.5-3 GPa, Green and Falloon, 2005). The other path is single inasmuch as, all things
539 (composition, flowing velocity, temperature, pressure) being equal, a more opened entrance angle of
540 mantle flux at a shorter distance from the ridge (500 km or less?) enables it to be mainly monitored by
541 the suction effect coming from the strongly depressurized shallow area below the spreading ridge.
542 This single path is assumed to be the one producing MORB after 15-20% melting between 65 and 45
543 km depth (2 to 1.6 GPa) (see section 5.1 below). Indeed at small-scale, we suggest that convective
544 eddies form by peeling off the upper surface of the lower asthenosphere and ascend driven by
545 buoyancy and rheology contrast with the upper asthenosphere. These ascending eddies would become
546 'isolated' or encapsulated by a cooling rind/skin as the temperature contrast increases between eddy
547 core and ambient mantle, forming diapirs. These eddies/diapirs move obliquely towards the shallow
548 area below the spreading ridge where they are tapped by fracturing at the rift.

549 "Eastward" of the ridge, because of the "westward" drift of the lithosphere, the suction effect fades
550 and mantle melting progressively mitigates top to bottom to become quite insignificant at more than
551 1000 km from the ridge. Accordingly in this model, off-axis melt lenses on the eastern side of the East
552 Pacific Ridge (Canales et al., 2012; Toomey, 2002, 2012) witness the asthenospheric partial melting
553 zone underlying the ridge just before eastward abandonment due to the westward migration of the
554 ridge.
555 According to this new scenario, the westward drift of the lithosphere and the related oceanic plate
556 spreading have a strong mechanical effect on lateral (several thousands kilometers long) and upward
557 (from 230 to 45 km depth) mantle mass transfer below the western plate A. This effect appears as
558 extremely relevant in terms of mass transfer and is synchronous with partial melting and
559 percolation/reaction processes, and thus mantle differentiation.
560 Therefore, as already inferred by Green et al. (2014) and Green (2015), the upper asthenosphere
561 mantle composition is heterogeneous at a small scale, being influenced from below by the ascending
562 lower asthenosphere and from above by the oceanic lithosphere during its journey and related process
563 of thickening. In other terms, from 230 km to 90-100 km, the upper asthenosphere should be a mantle
564 layer including incipient melt fractions coming from two distinct mantle sources: the lower
565 asthenosphere, the "dry" lherzolitic source of MORB on one hand; the lowermost part of lithosphere,
566 made of harzburgitic residues produced below the ridge axis, more (westward) or less (eastward)
567 refertilized and "wet" once accreted to the lithosphere.
568 All these data confirm that the asthenosphere forms a whole, 300-320 km thick, with a lower
569 "nearly dry" (~200 ppm H_2O) solid part (≈185 km thick; 2/3 in volume) and an upper "relatively wet
570 (> 200 ppm H_2O) solid + incipient melt" part (≈ 125 km thick; 1/3 in volume), the latter interacting
571 with the overlying lower lithosphere. The existence of the asymmetric LVZ below the oceans
572 indicates that below divergent plates, upwards and "eastward" transfer of lower asthenosphere is more
573 active than elsewhere, accelerating its replacement by eastward lateral mantle flow coming from
574 below the adjoining continents and related passive continental margin located to the "west" of a given
575 ocean. So before flowing below and interacting with oceanic lithosphere, the upper asthenosphere
576 underwent an earlier history of interaction with continental lithosphere, hence adding further chemical
577 heterogeneity to intraplate mantle sources.

578 **5. How to understand, within the framework of plate tectonics, the coexistence of mid-oceanic**
579 **basalt and oceanic intraplate basalt mantle sources within the asthenosphere?**

580 *5.1. Location of mid-oceanic basalt mantle sources*

581 Experimentally (Fig. 3), MORB are shown to be sourced from a roughly adiabatic (1490 to
582 1430°C) upwelling of the uppermost part (250-230 km) of lower asthenosphere with melt fraction
583 increasing dramatically above its anhydrous solidus (3 GPa/~100 km; 1450°C). MORB melt
584 segregation occurs at 15-20% melting between 2 and 1.6 GPa (65 to 45 km; Green and Falloon, 2005;
585 Falloon et al., 2007b) within the so called "melting area" below the ridge axis in our model (Fig. 2).
586 The MORB mantle source composition is lherzolitic and fertile in terms of mineral assemblage and
587 major element contents (Green and Falloon, 1998; 2005). However both trace element contents and
588 Nd-Sr-Pb isotopic signatures are those of a mantle depleted in the most incompatible trace elements,
589 *interpreted* as representative of a residual mantle composition. This decoupling between major and
590 trace element composition interpretations is explained considering that the MORB source is itself a
591 secondary lherzolite coming from the refertilization of a mantle residue by melts extracted from an
592 already trace element depleted lherzolitic mantle (Frey and Green, 1974; Piccardo et al., 2007), or an

593 eclogitic magmatic crust (Eller et al., 2000), or recycled components (e.g. oceanic crust, Eiler et al.,
594 2000; or metasomatized oceanic lithosphere, Niu et al. 2002; Shimizu et al., 2015), or a mix
595 (Rosenthal et al., 2014). So our model assumes that the uppermost part of the lower asthenosphere is a
596 secondary lherzolite, being the refertilization mostly provided from the recycling of W-directed
597 subducting oceanic lithospheric slabs (Rosenthal et al., 2014; Doglioni and Anderson, 2015; Green,
598 2015).
599 As shown by our model, the unique and unidirectional path of transfer of a mantle with a MORB
600 source signature, combined with the westward drift of the lithosphere and of the spreading ridge itself,
601 highlights the systematic and permanent identical replacement of the MORB mantle source within the
602 same P-T conditions of ascent and partial melting, which fits with the observed relative compositional
603 homogeneity of MORB (dominant N-MORB) through geological times. This compositional
604 homogeneity testifies itself for an absence of significant interactions of this oblique succession of
605 mantle diapirs (Green, 1971) crosscutting the surrounding upper asthenosphere, and therefore for the
606 relatively high velocity of such mantle diapirs driven by the suction effect of the spreading ridge.
607 Diapir buoyancy driven by density, rheology and isolation from wall-rock reaction, is probably more a
608 consequence of increasing temperature contrast if the diapir is near adiabatic i.e garnet lherzolite with
609 incipient melt into a rind of spinel lherzolite to plagioclase lherzolite (foliated to mylonitic).

610 *5.2. Location of oceanic intraplate basalt mantle sources*

611 As summarized by Green and Falloon (1998; 2005), Green et al. (2014), Green (2015) and Green
612 and Falloon (2015), intraplate magmas, including oceanic intraplate basalts (or "hot spots" basalts),
613 range from olivine melilitites and nephelinites, to olivine-rich basanites and finally to alkali basalts
614 and olivine tholeiites. Experimentally, these basalts represent low degree (2 to 10%) melts from
615 mantle sources located within the uppermost asthenosphere on 50 km thickness (≈ 110-160 km depth;
616 ≈ 3.3 to 5 GPa) or only 20 km thickness (≈ 105-125 km depth; ≈ 3 to 4 GPa) depending on the
617 considered geotherm ("intraplate" or "intraplate+ shear heating effect"; Fig. 3**)**. This upper
618 asthenospheric source mantle is lherzolitic as the MORB mantle source and thus fertile in terms of
619 mineral assemblage and major element contents, but above all rather enriched, and not depleted as the
620 MORB source, in water (> 0.02%) and in the most incompatible trace elements. As inferred in the
621 previous chapter, they are secondary lherzolites in which refertilization of mantle residues can have
622 two distinct origins. On one hand the lherzolites could derive from destabilization (≥ 90-100 km
623 depth) of the lowermost part of the subsiding oceanic lithosphere far from the axial ridge. This result
624 validates the hypothesis of an origin of some intraplate basalts from the lower lithospheric mantle in
625 terms of composition (Anderson, 2010, and references therein). In that case, mantle metasomatism
626 occurred below the spreading ridge by percolation/reaction of lithospheric mantle by MORB a rather
627 long time ago. On the other hand, these secondary lherzolites could derive from metasomatism of
628 lower asthenospheric material ascending throughout the upper asthenosphere along the main path with
629 a very low angle trajectory (Fig. 2; see § 4.2 for explanations). In that case, metasomatism results
630 from successive percolation/reaction of incipient melts with mantle constantly on the move laterally.
631 Nevertheless the Vs variations in the LVZ from one side to another of the ridge axis (cf. § 4.2)
632 suggests that the uppermost mantle fertility is somewhat reduced eastward.
633 Besides the Nd-Sr-Pb isotopic signatures of intraplate basalts attest for mantle sources also
634 metasomatized at some point in their long history by continental lithospheric products (Pilet et al.,
635 2005; 2008; 2011). Notice that most Pacific, but also Indian “hot spots” basalts (dominant alkali
636 intraplate basalts) are on the western or south-western plates relative to their respective axial ridges,
637 thus are sourced within the upper asthenosphere having previously interacted with western adjoining

638 and overlying continental plates. Such an interaction may be a candidate for explaining this
639 continental imprint on intraplate basalt mantle sources, coherently with the relative "eastward" mantle
640 flow.

641 **6. Towards an alternative oceanic plate spreading model for a polarized plate tectonics**

642 To date, a number of geophysical data at different scales demonstrate asymmetry of oceanic plates,
643 whereas mantle petrologists still conceive mantle differentiation as a symmetric process on both sides
644 of divergent plate boundaries and the underlying asthenosphere. To resolve this inconsistency,
645 combination of updated geophysical, structural and petrological data on oceanic upper mantle (down
646 to about 300 km) and also related concepts on mantle and magma genesis and plate kinematics, leads
647 to the development of an oceanic spreading model where both the growing oceanic lithospheric
648 mantle and the underlying upper asthenospheric mantle are to varying degrees asymmetric in
649 composition. Our model takes place in the frame of the westward drift of the lithosphere, which
650 means that oceanic ridges migrate laterally to the "west" relative to the asthenospheric mantle, and
651 thus are always moving over a fertile mantle.
652 From the geophysical data, the asymmetry concerns bathymetry of the ridge flanks (less steep
653 eastward), plate velocity rates (slower for the eastern one), thickness of plates (thinner eastward), and
654 faster shear wave velocity in the western lithosphere. It comes that plates on each side of the ridge
655 differ in density as well as rigidity, thus in composition, and thereby in growing conditions of mantle
656 lithosphere at the axial ridge.
657 To understand from a petrological but also kinematic point of view the aforementioned asymmetry,
658 mantle lithosphere and mantle asthenosphere were examined separately, even if they are
659 interdependent.
660 From natural and experimental data, three processes, two just below and one outside the spreading
661 ridge, are known to generate compositional heterogeneity of oceanic mantle lithosphere of both plates:
662 1) sub-ridge accretion of partial melting residues formed by melt segregation from mantle
663 asthenosphere upwelling; mantle lithosphere thickness at the axial ridge is estimated, via experimental
664 results on mantle phase equilibrium, between 30 to 80 km; 2) melt-rock reactions or mantle
665 metasomatism by basaltic melt percolation through previously accreted residues below the ridge,
666 inducing refertilisation and secondary lherzolite formation; 3) capture and addition of asthenospheric
667 mantle to the base of mantle lithosphere, because of cooling of the uppermost asthenosphere far from
668 the ridge. This last process occurs when the geotherm drops below 1050°C at 3 GPa which yields a
669 LAB at ~90km below which neither pargasite or hydrous carbonate-bearing silicate melt could exist.
670 It gives a thickened lithosphere with the growing layer of subsolidus phlogopite-bearing garnet-
671 lherzolite with carbonatite, or graphite+ H_2O+CH_4 fluid.
672 Structural data released by mapping numerous mantle core complexes, mostly immediately
673 westward of active slow-spreading ridges, give strong structural constraints for understanding
674 lithospheric mantle dynamics during plate spreading. Indeed whether in the west or east, these core
675 complexes represent outcrops of mantle and related intrusive gabbro bodies exhumed along the
676 footwall of convex up-wards detachment faults dipping eastward and rooted down to 7-8 km. We
677 interpret these detachment faults as effects of top to bottom asymmetric lithospheric mantle shear,
678 linked to the eastward flowing of asthenosphere delaying the base of the lithosphere moving
679 westward. The usual sill shape of gabbro intrusive bodies is another observation supporting intra-
680 mantle decoupling during ocean spreading. Furthermore, at the topmost part of the hangingwall of
681 these large detachment faults, a small-scale decoupling occurs between the base of volcanoes and
682 underlying mantle or/and gabbro bodies in process of exhumation, underlining this time a pseudo-

683 symmetric spreading. It follows that whatever the scale, the top to bottom decoupling dynamics
684 enables the exhumation of deep rocks (mantle with or without intrusive gabbro), thus the creation of
685 new surfaces, giving all its meaning to the concept of "detachment-mode of seafloor spreading"
686 developed by Maffione et al (2013). *This top to bottom mantle decoupling preserves totally magnetic*
687 *anomalies recorded at the surface on each side of the axis.*
688 Considering all these results, the mantle lithosphere composition can evolve differently on each
689 side of the ridge, coming from a permanent refertilisation of the western plate whereas the eastern
690 plate just preserves the barely refertilized feature of a harzburgitic residue generated during
691 asthenosphere partial melting below axial ridge. So rigidity, density to a lesser extent and thickness of
692 the western plate become much higher, whereas the shallower bathymetry of the east flank of the
693 ridge is explained by isostatic adjustment because of a somewhat lower density. Also as the eastern
694 plate mantle is lighter and more viscous, there is a higher coupling at the lithosphere-asthenosphere
695 boundary, determining a slower velocity of the eastern plate during ridge migration. The top to bottom
696 and west to east internal decoupling of the mantle lithosphere, linked to its westward drift above the
697 asthenospheric mantle flowing eastward, explains detachment faults and related mantle core complex
698 exhumation.
699 The petrology of asthenospheric mantle is known experimentally since asthenosphere is the mantle
700 reservoir, at distinct P-T-depths, of MORB (lower asthenosphere) and intraplate basalts (middle to
701 upper asthenosphere). An asymmetric "incipient melt + solid" mantle zone, the LVZ, exists between
702 230 and 100 km, being much more developped and more fertile westward. So MORB are sourced
703 from a lherzolitic mantle in equilibrium at ≈ 250-230 km / 7 GPa, the ascent of which up to 65-45 km
704 / 2-1.6 GPa just below the ridge is roughly adiabatic, thus rather fast and without any significant
705 interaction with surrounding crosscut upper asthenosphere. According to the relative “eastward”
706 direction of the asthenospheric mantle flow lines, the diapiric rise of MORB mantle source from lower
707 asthenosphere is significantly oblique and eastward. This mantle transfer is triggered and checked by
708 the suction effect of the spreading ridge, and the westward ridge migration determines a self-
709 perpetuating mechanism for permanently renewing the MORB source mantle, which explains in
710 return the great homogeneity of MORB through time. Synchronously, major mantle transfers within
711 middle to upper asthenosphere come from the lower asthenosphere farther westward and follow the
712 eastward mantle flow lines, slightly slantwise but barely deviated by the suction effect of the
713 spreading ridge. Mantle undergoes incipient melting, except that the interstitial melts percolate
714 laterally and upwards, react with and enrich the upper asthenosphere in water and the most
715 incompatible elements, a possible mantle reservoir for intraplate basalts. This incipient melting zone
716 represents also the lithosphere-asthenosphere decoupling zone affected by shear heating, reducing the
717 P/depth of intraplate magma genesis. Also the higher shear wave velocity eastward means a density
718 decrease in relation with a somewhat residual feature of the eastern asthenospheric mantle and
719 reflecting a mixing with residual mantle coming from the high degree melting area below the ridge
720 and not accreted to the lithosphere.

721 **7. Conclusions**

722 The proposed oceanic plate spreading model shows that numerous asymmetric features observed
723 with geophysics and structural analysis in the first 300 km below the oceans are consistent with
724 petrological data on upper mantle and basaltic compositions. Our multi-disciplinary study emphasizes
725 the major role of physical and chemical dynamics of the upper mantle for understanding oceanic plate
726 tectonics, and in turn how evolution of both the composition and internal structure of oceanic plates
727 strongly depends at all scales on plate kinematics. Our model suggests that both plate composition and

728 kinematics are interdependent on asthenosphere compositional evolution. The spreading of an ocean,
729 synchronous with the migration of the mid-oceanic ridge, induces a complete and permanent material
730 renewal, by mass transfer at all scales, particularly in the shallow 300 km of the Earth's mantle below
731 the whole width of the oceans. Another major concept is that all petrological processes, occurring
732 during different types of solid or/and liquid mantle mass transfers, ultimately lead to the genesis of a
733 more or less fertile mantle composition, i.e. a lherzolite but secondary in nature (residual harzburgite
734 refertilized by melt interaction), which is the main composition of the first 300 km of the Earth below
735 oceans and most likely the continents as well. Incompatible trace elements abundances and isotopic
736 values of mantle sources will necessarily vary from one specific mantle site to another reflecting the
737 detailed individual geological histories of 'lherzolites'.

738 **Acknowledgments**

739 We are grateful for fruitful and helpful discussions to David H. Green, Don Anderson, Eugenio
740 Carminati, Marco Cuffaro and Giuliano Panza. F. Chalot-Prat is grateful to the CRPG for its financial
741 support to allow brainstorming meetings between the authors of this paper. We gratefully
742 acknowledge David H. Green for his thorough, very constructive and interesting review that helped us
743 to deepen our observations and our model, and to an anonymous reviewer for his numerous pertinent
744 remarks and his careful and patient work on the form of the text, usefully clarifying the content and
745 form of this multi-disciplinary study. Our warm thanks go to Marco Scambelluri for his extensive
746 work during the reviewing process and all his attention as editor of this paper. The data used are listed
747 in the references. This is the CRPG-CNRS contribution no. 2433.

748 **References**

749 Abily, B., Ceuleneer G. 2013. The dunitic mantle-crust transition zone in the Oman ophiolite: Residue
750 of melt-rock interaction, cumulates from high-MgO melts, or both? Geology, 41, 67-70.
751 Doi :10.1130/G33351.1
752 Afonso, J. C., Fernandez M., Ranalli G., Griffin W. L., Connolly J. A. D. 2008. Integrated
753 geophysical-petrological modeling of the lithosphere and sublithospheric upper mantle:
754 Methodology and applications, Geochem. Geophys. Geosyst., 9, Q05008,
755 doi:10.1029/2007GC001834.
756 Anderson, D.L., 2007. New Theory of the Earth, Cambridge University Press.
757 Anderson, D.L., 2010. Hawaii, boundary layers and ambient mantle-geophysical constraints. J.
758 Petrology, doi: 10.1093/petrology/egq068.
759 Bonatti, E., Ligi M., Brunelli D., Cipriani A., Fabretti P., Ferrante V., Ottolini L. 2003. Mantle
760 thermal pulses below the Mid Atlantic Ridge and temporal variations in the oceanic
761 lithosphere, Nature, 423, 499–505.
762 Bostrom, R.C., 1971. Westward displacement of the lithosphere. Nature 234, 536–538.
763 Brune S., Heine, C., Pérez-Gussinye M., Sobolev S.V. 2014. Rift migration explains continental
764 margin asymmetry and crustal hyper-extension. Nature Communications, 5:4014,
765 doi:10.1038/ncomms5014.
766 Canales, J.P., Carton, H., Carbotte, S. M., Mutter, J.C., Nedimovi´c, M.R., Xu, M., Aghaei, O.,
767 Marjanovi´c, M., Newman, K., 2012. Network of off-axis melt bodies at the East Pacific
768 Rise. Nature Geoscience, 5, 279-283.
769 Cannat, M., 1993. Emplacement of mantle rocks in the seafloor at mid-ocean ridges. Journal of
770 Geophysical Research, Solid Earth, 98, B3, 4163–4172.

771 Carbotte, S.M., Small C. Donnelly K. 2004. The influence of ridge migration on the magmatic
772 segmentation of mid–ocean ridges, Nature, 429, 743–746.
773 Carey, S.W., 1958. Continental Drift—A symposium (Univ. of Tasmania, Hobart, March 1956), 177–
774 363.
775 Chalot-Prat, F, 2005. An undeformed ophiolite in the Alps: field and geochemical evidences for a link
776 between volcanism and shallow plate tectonic processes. In Plates, Plumes & Paradigms,
777 edited by G.R. Foulger, D.L. Anderson, J.H. Natland and D.C. Presnall, Geological Society
778 of America, Special Paper 388, 751–780.
779 Chalot-Prat, F., Falloon T. J., Green D. H. Hibberson W. O., 2010. An experimental study of liquid
780 compositions in equilibrium with plagioclase+spinel lherzolite at low pressures (0·75GPa).
781 Journal of Petrology, 51(11), 23–49-2376.
782 Chalot-Prat, F., Falloon T. J., Green D. H., Hibberson W. O., 2013. Melting of plagioclase + spinel
783 lherzolite at low pressures (0.5 GPa): An experimental approach to the evolution of basaltic
784 melt during mantle refertilisation at shallow depths. Lithos, 172-173, 61–80.
785 Conder, J.A., Wiens, D.A., 2006. Seismic structure beneath the Tonga arc and Lau backarc basin
786 determined from joint Vp, Vp/Vs tomography. Geochemistry, Geophysics, Geosystems 7,
787 Q03018.
788 Crespi, M., Cuffaro, M., Doglioni, Giannone, C., Riguzzi, F., 2007. Space geodesy validation of the
789 global lithospheric flow. Geophysical Journal International, 168, 491-506, doi:
790 10.1111/j.1365-246X.2006.03226.x.
791 Cuffaro, M., Doglioni, C., 2007. Global kinematics in deep versus shallow hotspot reference frames,
792 In: Foulger, G.R., and Jurdy, D.M. (Eds.), Plates, plumes, and planetary processes:
793 Geological Society of America Special Paper 430, 359–374, doi: 10.1130/2007.2430(18).
794 Dijkstra, A.H., Drury, M.R., Visser, L.R.M., 2001. Structural petrology of plagioclase peridotite in the
795 West Othris mountains (Grece): melt impregnation in mantle lithosphere. Journal of
796 Petrology 42, 5–24.
797 Dick, H.J.B., Natland, J.H. 1996. Late-stage melt evolution and transport in the shallow mantle
798 beneath the East Pacific Rise, in Mével, C., et al., eds. Proceedings of the Ocean Drilling
799 Program, Scientific Results, 147:College Station, Texas, Ocean Drilling Program, 103–134.
800 Doglioni, C., Carminati, E., Bonatti, E., 2003. Rift asymmetry and continental uplift. Tectonics, 22,
801 1024-1037, doi:10.1029/2002TC001459
802 Doglioni, C., Carminati, E., Cuffaro, M., Scrocca, D., 2007. Subduction kinematics and dynamic
803 constraints. Earth Science Reviews, 83, 125-175, doi:10.1016/j.earscirev.2007.04.001.
804 Doglioni, C., Green, D.H., Mongelli, F., 2005. On the shallow origin of hotspots and the westward
805 drift of the lithosphere. In: Foulger, G.R., Natland, J.H., Presnall, D.C., and Anderson, D.L.
806 (Eds.), Plates, plumes, and paradigms: Geological Society of America Special Paper 388,
807 735–749, doi: 10.1130/2005.2388(42).
808 Doglioni, C., Ismail-Zadeh, A., Panza, G., Riguzzi, F. 2011. Lithosphere-asthenosphere viscosity
809 contrast and decoupling, Physics of the Earth and Planetary Interiors, 189, 1-8.
810 Doglioni, C., Anderson, D.L., 2015. Top driven asymmetric mantle convection. In The
811 Interdisciplinary Earth: A volume in honor of Don L. Anderson. Geological Society of
812 America Special Paper 514, American Geophysical Union Special Publication 71,
813 doi:10.1130/2015.2514(05).
814 Doglioni, C., Panza, G.F., 2015. Polarized plate tectonics. Advances in Geophysics, 56, 3, 1-167,
815 http://dx.doi.org/10.1016/bs.agph.2014.12.001

816 Eggins, S. M., 1992a. Petrogenesis of Hawaiian tholeiites: 1. Phase equilibria constraints.
817 Contributions to Mineralogy and Petrology 110, 387-397.
818 Eggins, S. M., 1992b. Petrogenesis of Hawaiian tholeiites: 2. Aspects of dynamic melt segregation.
819 Contributions to Mineralogy and Petrology110, 398-410.
820 Eiler J.M., Schiano, P., Kitchen, N., Stolper E.M., 2000. Oxygen-isotope evidence for recycled crust
821 in the sources of mid-ocean-ridge basalts. nature, 403, 530-534.
822 Falloon, T. J., Danyushevsky, L. V., Ariskin, A., Green, D. H., 2007a. The application of olivine
823 geothermometry to infer crystallization temperatures of parental liquids: implications for the
824 temperature of MORB magmas. Chemical Geology 241, 207^233.
825 Falloon, T.J., Green, D.H. Danyushevsky, L.V. 2007b. Crystallization temperatures of tholeiite
826 parental liquids: Implications for the existence of thermally driven mantle plumes, in
827 Foulger, G.R., and Jurdy, D.M., eds., Plates, plumes, and planetary processes: Geological
828 Society of America Special Paper 430, 235–260, doi:10.1130/2007.2430(12)
829 Frey, F.A., Green, D. H., 1974. The mineralogy, geochemistry and origin of lherzolite inclusions in
830 Victorian basanites. Geochimica et Cosmochimica Acta, 38, 1023-1059.
831 Fyfe, W.S., 1960. The possibility of *d*-electron coupling in olivine at high pressures. Geochimica et
832 Cosmochimica Acta, 19, 141-143.
833 Green, D. H., 1971. Composition of basaltic magmas as indicators of conditions of origin: application
834 to oceanic volcanism. Philosophical Transactions of the Royal Society of London, A 268,
835 707-725.
836 Green, D. H., Falloon, T. J., 1998. Pyrolite: A Ringwood concept and its current expression. In:
837 Jackson INS (ed) The Earth's mantle: composition, structure and evolution. Cambridge
838 University Press, Cambridge, pp 311–380.
839 Green, D. H., Falloon, T. J., Eggins, S. M., Yaxley, G. M., 2001. Primary magmas and mantle
840 temperatures. European Journal of Mineralogy 13(3), 437-451.
841 Green, D. H., Falloon, T. J., 2005. Primary magmas at mid-ocean ridges, 'hotspots', and other
842 intraplate settings: Constraints on mantle potential temperature. In: Foulger, G. R., Natland,
843 J. H., Presnall, D. C. & Anderson, D. L. (eds) Plates, Plumes, and Paradigms. Geological
844 Society of America, Special Papers 388, 217-247.
845 Green, D. H., Falloon, T. J., (2015), Mantle-derived magmas: intraplate, hot-spots and mid-ocean
846 ridges, Sci. Bull. , doi:10.1007/s11434-015-0920-y
847 Green, D.H., Hibberson, W.O., Kovacs, I., Rosenthal, A., 2010. Water and its influence on the
848 lithosphere – asthenosphere boundary. Nature 467, 448–451. doi:10.1038/nature09369.
849 Green, D.H., Hibberson, W.O., Kovacs, I., Rosenthal, A., 2011. Water and its influence on the
850 lithosphere-asthenosphere boundary, 467, 448-451, 2010). [Addendum.]. Nature 472(7344),
851 504.
852 Green, D.H., Hibberson, W.O., Rosenthal, A., Kovacs, I., Yaxley, G.M., Falloon, T.J., Brink, F. 2014.
853 Experimental study of the influence of water on melting and phase assemblages in the upper
854 mantle. Journal of Petrology, 55, 10, 2067-2096 doi: 10.1093/petrology/egu050.
855 Green, D.H., 2015. Experimental petrology of peridotites, including effects of water and carbon on
856 melting in the Earth's uppermantle. Phys Chem Miner 42, 95–102. doi: 10.1007/s00269-
857 014-0729-2.
858 Gripp, A.E., Gordon, R.G., 2002. Young tracks of hotspots and current plate velocities: Geophysical
859 Journal International, v. 150, p. 321–364, doi: 10.1046/j.1365-246X.2002.01627.x.
860 Hammond, W. C., Toomey, D. R., 2003. Seismic velocity anisotropy and heterogeneity beneath the
861 Mantle Electromagnetic and Tomography Experiment (MELT) region of the East Pacific

862 Rise from analysis of P and S body waves, Journal of Geophysical Research, 108, 2176, doi:
863 10.1029/2002JB001789, B4.
864 Henstock, T. J., Woods, A. W., White, R. S., 1993. The accretion of oceanic crust by episodic sill
865 intrusion. Journal of Geophysical Research, Solid Earth, 98, 4143–4161.
866 Harper, G. D., 1985. Tectonics of slow spreading mid-ocean ridges and consequences of a variable
867 depth to the brittle/ductile transition. Tectonics, 4(4), 395-409. doi:
868 10.1029/TC004i004p00395.
869 Holmes, A., 1944. Principles of physical geology. In Thomas Nelson and Sons LTD, Edinburgh (ed.).
870 Jordan, T. H., 1979. Mineralogies, densities and seismic velocities of garnet lherzolites and their
871 geophysical implications, in The Mantle Sample: Inclusion in Kimberlites and Other
872 Volcanics (eds F.R. Boyd and H. O.A. Meyer), American Geophysical Union, Washington
873 D.C. 1-13. doi: 10.1029/SP016p0001
874 Kaczmarek, M.A., Müntener, O., 2008. Juxtaposition of melt impregnation and high temperature
875 shear zones in the upper mantle; field and petrological constraints from the Lanzo peridotite
876 (Northern Italy). Journal of Petrology 49, 2187–2220.
877 Kaczmarek, M.A., Müntener, O., 2010. The variability of peridotite composition across a mantle shear
878 zone (Lanzo massif, Italy): interplay of melt focusing and deformation. Contribution to
879 Mineralogy and Petrology 160, 663–679
880 Lavier, L. L., Manatschal, G., 2006. A mechanism to thin the continental lithosphere at magma-poor
881 margins. Nature 440, 324–328.
882 Le Pichon, X., 1968. Sea-floor spreading and continental drift. Journal of Geophysical Research, 73,
883 12, 3661-3697.
884 Ligi, M., Bonatti, E., Cipriani, A., Ottolini, L., 2005. Water-rich basalts at mid-ocean-ridge cold spots.
885 Nature, 434, 7029, 66-69.
886 MacLeod, C.J., Searle, R.C., Murton, B.J., Casey, J.F., Mallows, C., Unsworth, S.C., Achenbach,
887 K.L., Harris, M., 2009. Life cycle of oceanic core complexes. Earth and Planetary Science
888 Letters 287,333–344
889 Maffione, M., Morris, A., Anderson, M.W., 2013. Recognizing detachment-mode seafloor spreading
890 in the deep geological past. Scientific report 3, 2336, doi: 10.1038/srep02336.
891 Mallows, C., Searle, R. C., 2012. A geophysical study of oceanic core complexes and surrounding
892 terrain, Mid-Atlantic Ridge 13_N–14_N, Geochem. Geophys. Geosyst., 13, Q0AG08,
893 doi:10.1029/2012GC004075.
894 Moore, G.W., 1973. Westward tidal lag as the driving force of plate tectonics. Geology, 1, 99–100.
895 Müller, R.D., Roest, W.R., Royer, J.Y., Gahagan, L.M., Sclater, J.G., 1997. Digital isochrons of the
896 world's ocean floor, Journal of Geophysical Research, 102, 3211–3214.
897 Müller, R.D., Sdrolias, M., Gaina, C., Roest, W.R., 2008. Age, spreading rates, and spreading
898 asymmetry of the world's ocean crust, Geochemistry, Geophysics, Geosystems, 9, Q04006,
899 doi:10.1029/2007GC001743.
900 Müntener, O., Pettke, T., Desmurs, L., Meier, M., Schaltegger, U., 2004. Refertilization of mantle
901 peridotite in embryonic ocean basins: trace element and Nd-isotope evidence and
902 implications for crust-mantle relationships, Earth and Planetary Science Letters 221, 293–
903 308.
904 Muntener, O., Manatschal, G., Desmurs, L., Pettke T., 2010. Plagioclase peridotites in ocean-
905 continent transitions: Refertilized mantle domains generated by melt stagnation in the
906 shallow mantle lithosphere, Journal of Petrology, 51, 255-294.

907 Niu, Y. L., Regelous, M., Wendt, I. J., Batiza, R. and O'Hara, M. J., 2002. Geochemistry of near-EPR
908 seamounts: importance of source vs. process and the origin of enriched mantle component.
909 Earth Planetary Science Letters, 199, 327–345.
910 Panza, G.F., Doglioni, C., Levshin, A., 2010. Asymmetric ocean basins, Geology, 38, 1, 59-62. doi:
911 10.1130/G30570.1.
912 Panza, G.F., Romanelli, F., 2014. Seismic waves in 3-D: from mantle asymmetries to reliable seismic
913 hazard assessment. Earthq Sci 27(5), 567–576, doi:10.1007/s11589-014-0091-y.
914 Piccardo, G.B., Müntener, O., Zanetti, A., Pettke, T., 2004. Ophiolitic peridotites of the Alpine-
915 Apennine system: mantle processes and geodynamic relevance, International Geology
916 Review 46, 1119–1159
917 Piccardo, G.B., Poggi, E., Vissers, R.L.M., 2007a. The pre-oceanic evolution of the Erro–Tobbio
918 peridotite (Voltri Massif, Ligurian Alps, Italy), Journal of Geodynamics 43, 417–449.
919 Piccardo, G.B., Zanetti, A., Müntener, O., 2007b. Melt/peridotite interaction in the Southern Lanzo
920 peridotite: field, textural and geochemical evidence. Lithos 94, 181–209.
921 Piccardo, G.B., Guarnieri, L. 2010. The Monte Maggiore peridotite (Corsica, France): a case study of
922 mantle evolution in the Ligurian Tethys. Geological Society, London, Special Publications,
923 337, 7-45, doi:10.1144/SP337.2
924 Piccardo, G.B., M. Padovano, and L. Guarnieri (2014), The ligurian tethys: mantle processes and
925 geodynamics. Earth-Science Reviews, 138, 409–434, doi:10.1016/j.earscirev.2014.07.002.
926 Pilet, S., Baker, M.B., and Stolper, E.M., 2008. Metasomatized lithosphere and the origin of alkaline
927 lavas, Science, 320, 916-919.
928 Pilet, S., Baker, M.B., Muntener, O. Stolper, E. M., 2011. Monte Carlo simulations of metasomatic
929 enrichment in the lithosphere and implications for the source of alkaline basalts, Journal of
930 Petrology, 52, 1415-1442.
931 Pilet, S., Hernandez, J., Sylvester, P., Poujol, M., 2005. The metasomatic alternative for ocean island
932 basalt chemical heterogeneity, Earth and Planetary Science Letters, 236, p. 148-166.
933 Rampone, E., Borghini, G., 2008. The melt intrusion/interaction history of the Erro–Tobbio
934 peridotites (Ligurian Alps, Italy): insights on mantle processes at nonvolcanic passive
935 margins. European Journal of Mineralogy 20, 573–585.
936 Rampone, E., Piccardo, G.B., Hofmann, A.W., 2008. Multi-stage melt-rock interaction in the Mt.
937 Maggiore (Corsica, France) ophiolitic peridotites: microstructural and geochemical records.
938 Contribution to Mineralogy and Petrology 156, 453–475.
939 Rampone, E., Piccardo, G.B., Vannucci, R., Bottazzi, P., 1997. Chemistry and origin of trapped melts
940 in ophiolitic peridotites. Geochimica et Cosmochimica Acta 61, 4557–4569.
941 Rampone, E., Romairone, A., Abouchami, W., Piccardo, G.B., Hofmann, W., 2005. Chronology,
942 petrology and isotope geochemistry of the Erro–Tobbio peridotites (Ligurian Alps, Italy):
943 records of late Palaeozoic lithospheric extension, Journal of Petrology 46, 799–827.
944 Rampone, E., Hofmann, A.W., 2012. A global overview of isotopic heterogeneities in the oceanic
945 mantle, Lithos 148, 247–261.
946 Reston, T. J., Ranero, C. R., 2011. The 3-D geometry of detachment faulting at mid-ocean ridges,
947 Geochem. Geophys. Geosyst., 12, Q0AG05, doi:10.1029/2011GC003666.
948 Ricard, Y., Doglioni, C., Sabadini, R., 1991. Differential rotation between lithosphere and mantle: A
949 consequence of lateral mantle viscosity variations, Journal of Geophysical
950 Research, 96(B5), 8407–8415, doi:10.1029/91JB00204.
951 Riguzzi, F., Panza, G., Varga, P. Doglioni, C., 2010. Can Earth's rotation and tidal despinning drive
952 plate tectonics? Tectonophysics, 484, 60-73. doi:10.1016/j.tecto.2009.06.012.

953 Scoppola, B., Boccaletti, D., Bevis, M., Carminati, E., Doglioni, C., 2006. The westward drift of the
954 lithosphere: a rotational drag? Geological Society of America Bulletin, 118, 199–209,
955 doi:10.1029/2004TC001634.
956 Rosenthal, A., Yaxley, G.M., Green, D. H., Hermann, J., Kovacs, I., Spandler, C., 2014. Continuous
957 eclogite melting and variable refertilisation in upwelling heterogeneous mantle, Scientific
958 Reports 4, 6099, 10.1038/srep06099.
959 Scheirer, D.S., Forsyth, D.W., Cormier, M.H., Macdonald, K.C., 1998. Shipboard geophysical
960 indications of asymmetry and melt production beneath the East Pacific Rise near the MELT
961 experiment: Science, 280, 1221–1224, doi: 10.1126/science.280.5367.1221.
962 Shen, Y., Forsyth, D.W., Scheirer, D.S., Macdonald, K.C., 1993. Two forms of volcanism:
963 implications for mantle flow and off-axis crustal production on the west flank of the
964 southern east pacific rise. Journal of Geophysical Research 98, B10, 17,875-17,889.
965 Shimizu, K., Saal, A.E., Myers, C.E., Nagle, A.N., Hauri, E.H., Forsyth, D.W., Kamenetsky, V.S.,
966 Niu, Y., 2016. Two-component mantle melting-mixing model for the generation of mid-
967 ocean ridge basalts: Implications for the volatile content of the Pacific upper mantle.
968 Geochimica et Cosmochimica Acta, 176, 44–80.
969 Schmerr, N., 2012. The Gutenberg discontinuity: Melt at the lithosphere-asthenosphere boundary,
970 Science 335, 14801483.
971 Seyler, M., Bonatti, E., 1997. Regional-scale melt-rock interaction in lherzolitic mantle in the
972 Romanche fracture zone (Atlantic Ocean), Earth and Planetary Science Letters 146, 273–
973 287.
974 Small, C., Danyushevsky L. 2003. A plate kinematic explanation for mid-ocean ridge depth
975 discontinuities, Geology, 31, 399-402.
976 Smith, D.K., Escartín, J., Schouten, H., Cann, J.R., 2008. Fault rotation and core complex formation:
977 Significant processes in seafloor formation at slow-spreading mid-ocean ridges (Mid-
978 Atlantic Ridge, 13_–15_N), Geochem. Geophys. Geosyst., 9(3), 10.1029/2007GC001699
979 Smith, D.K., Escartín, J., Schouten, H., Cann, J.R., 2012. Active long-lived faults emerging along
980 slow-spreading mid-ocean ridges, Oceanography 25(1), 94–99,
981 http://dx.doi.org/10.5670/oceanog.2012.07.
982 Tartarotti, P., Susini, S., Nimis, P., Ottolini, L., 2002. Melt migration in the upper mantle along the
983 Romanche fracture zone (Equatorial Atlantic). Lithos 63, 125–149.
984 Takahashi, N., (2001), Origin of Plagioclase Lherzolite from the Nikanbetsu Peridotite Complex,
985 Hokkaido, Northern Japan: Implications for Incipient Melt Migration and Segregation in the
986 Partially Molten Upper Mantle. Journal of Petrology 42, 39-54.
987 Thybo, H., 2006. The heterogeneous upper mantle low velocity zone. Tectonophysics 416, 53–79.
988 Toomey D.R., Wilcock, W.S.D., Conder, J.A., Forsyth, D.W, Blundy, J.D., Parmentier, E.M.,
989 Hammond, W.C., 2002. Asymmetric mantle dynamics in the MELT region of the East
990 Pacific Rise. Earth and Planetary Science Letters 200, 287–295.
991 Toomey D.R., 2012. Piecing together rifts. Nature Geoscience 5, 235–236.
992 Vine, F. J., Matthews, D. H., 1963. Magnetic Anomalies Over Oceanic Ridges, Nature, 199(4897),
993 947–949. doi: 10.1038/199947a0.
994 Warren, J.M., Shimizu, N., 2010. Cryptic variations in abyssal peridotite compositions: evidence for
995 shallow-level melt infiltration in the oceanic lithosphere. Journal of Petrology 51, 395–423.
996 Warren, J.M., 2016. Global variations in abyssal peridotite compositions. Lithos, 248-251, 193-219.
997 Wegener, A., 1915. Die Entstehung der Kontinente und der Ozeae: Samml. Vieweg, Braunschweig,
998 23, pp 1-94.

White, S.C., Macdonald, K.C., Scheirer, D.S., Cormier, M.H., 1998. Distribution of isolated volcanoes on the flanks of the East Pacific Rise, 15.3°S-20°S. Journal of Geophysical Research 103, B12, 30,371-30,384.

Whitney, D. L., Teyssier, C., Rey, P., Buck, W. R., 2013. Continental and oceanic core complexes, GSA Bulletin, 125, 3/4, 273–298, doi: 10.1130/B30754.1.

Figure captions

Figure 1. Uninterpreted (above) and interpreted (below). Shear wave velocity (Vs) sections along the tectonic equator (TE) for the Earth's first 300 km. The mantle is faster and the lithosphere is thicker in the western side with respect to the eastern side of the three major oceanic ridges, EPR—Eastern Pacific Ridge, MAR—Mid-Atlantic Ridge, IR—Indian Ridge. Upper asthenosphere superposes to low-velocity layer (LVZ), i.e., which is the main decoupling surface between lithosphere and mantle, allowing net rotation of lithosphere, i.e., a first-order eastward relative mantle flow, or westward drift of lithosphere. Secondary flow should be related to mantle obliquely upraised along oceanic ridges. Asymmetry between two sides of ridges is independent from age of oceanic lithosphere, shown at top in million years (modified after Panza et al., 2010).

Figure 1

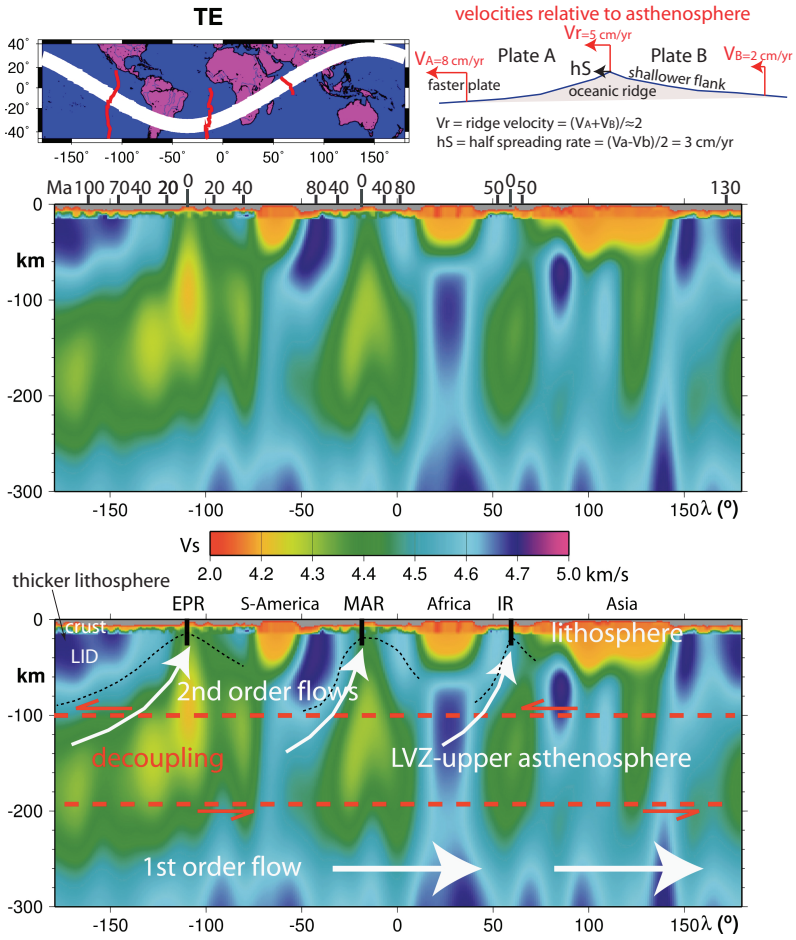

Figure 2. Inferred kinematics of different particles of mantle rocks along a migrating mid-oceanic ridge, and related asymmetric upper mantle differentiation. Numbers from 1 to n indicate progressive age evolution of the rock markers within lithosphere and asthenosphere. Plates A and B move with velocity VA and VB, respectively. Vr is the velocity of the ridge; hS is the half-spreading rate. Since the ridge is moving westward, new sections of asthenospheric mantle migrate "eastward" relative to the lithosphere, permanently renewing mantle source of isostatically upwelling magma generated by depressurization below the ridge. During this mass transfer, the eastern part of upper asthenosphere becomes somewhat Fe-depleted, while a top to bottom mantle path decoupling occurs due to the relative "westward" drift of overlying lithosphere. The upper asthenosphere (LVZ) corresponds to the oblique ascent of partially molten mantle from lower asthenosphere. Two different paths of transfer exist: the main one (yellow paths) barely deviated in passing below the ridge, the other (red path) monitored by the suction effect from the strongly depressurized area below the spreading ridge and giving MORB (see Fig. 3 for details). Mantle lithosphere is created at the ridge through accretion of residues above the asthenospheric partial melting area, residues successively transferred upwards and laterally at hS rate within the mantle lithosphere on each side of the ridge. A top to bottom decoupling exists within the mantle lithosphere linked to the slow-down by the eastward underlying flow of asthenosphere, and is responsible for detachment faults and mantle exhumation at the spreading ridge. Besides the mantle lithosphere composition, different on each side of the ridge, comes from a permanent refertilisation of the western plate whereas the eastern plate just preserves the barely refertilized feature of a harzburgitic residue generated during asthenosphere partial melting below axial ridge. See text for more details.

Figure 2

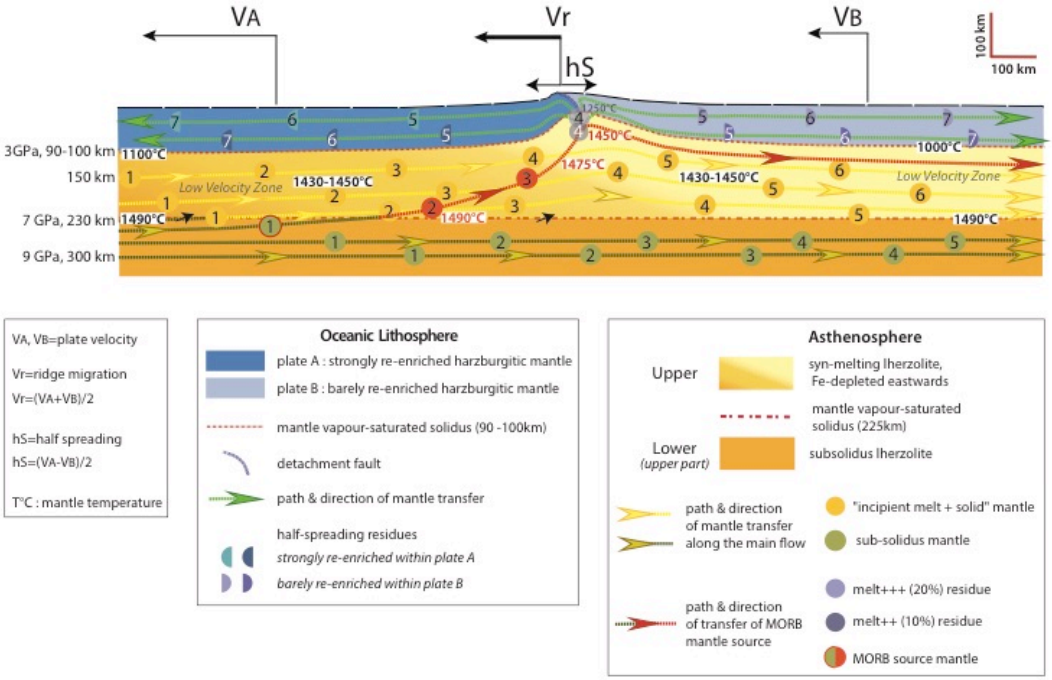

Figure 3. P-T-H_2O diagrams, modified from Fig. 6 in *Green et al.* 2014. a) Experimentally determined solidi for hydrous silicate melt in fertile lherzolite for different water contents; *blue dashed line*: mantle adiabat; *red star*: MORB source mantle upwelling potential temperature at 230, 150, 105 and 65 km; *green dashed line*: intraplate geotherm; *orange dotted line:* perturbation of oceanic intraplate geotherm by shear heating, adapted from Fig. 4 in *Doglioni et al.* 2005; *orange dot*: intraplate magma genesis at shallower depths (105 to 125 km vs. 110 to 160 km) taking into account shear heating within the lithosphere - asthenosphere decoupling zone. MORB are sourced from upwelling trace element depleted lherzolite from lower asthenosphere. Intraplate basalts, including OIB, are the products of upwelling of trace element enriched lherzolite from the middle and upper asthenosphere. See text for more details. b) Water storage capacity of lherzolitic mantle as a function of depth along the vapour-saturated solidus. Pargasite becomes unstable at >3 GPa, and water storage capacity drops to that (~200 ppm) which can be retained in NAMs (nominally anhydrous minerals) in lherzolite, inducing incipient melting of upper asthenosphere (LVZ). See text for more details.

Figure 3